# Lack of aprataxin impairs mitochondrial functions via downregulation of the APE1/NRF1/NRF2 pathway

Beatriz Garcia-Diaz[1], Emanuele Barca[1,3], Andrea Balreira[1], Luis C. Lopez[1,4], Saba Tadesse[1], Sindhu Krishna[2], Ali Naini[2], Caterina Mariotti[5], Barbara Castellotti[5] and Catarina M. Quinzii[1,*]

[1]Department of Neurology, [2]Department of Pathology and Cell Biology, Columbia University Medical Center, New York, NY 10032, USA, [3]UOC of Neurology and Neuromuscular Disorders, Department of Neuroscience, University of Messina, Messina 98100, Italy, [4]Institute of Biotechnology, Biomedical Research Center (CIBM), Health Science Technological Park (PTS), University of Granada, Armilla, Granada 18100, Spain and [5]Unitâ di Genetica delle Malattie Neurodegenerative e Metaboliche, Fondazione IRCCS Istituto Neurologico 'Carlo Besta', Milan 20126, Italy

*To whom correspondence should be addressed at: Columbia University Medical Center, 630 W 168th Street, P&S 4-431, New York, NY 10032, USA. Tel: +1 2123051048; Fax: +1 2123053986; Email: cmq2101@cumc.columbia.edu

## Abstract

Ataxia oculomotor apraxia type 1 (AOA1) is an autosomal recessive disease caused by mutations in APTX, which encodes the DNA strand-break repair protein aprataxin (APTX). $CoQ_{10}$ deficiency has been identified in fibroblasts and muscle of AOA1 patients carrying the common W279X mutation, and aprataxin has been localized to mitochondria in neuroblastoma cells, where it enhances preservation of mitochondrial function. In this study, we show that aprataxin deficiency impairs mitochondrial function, independent of its role in mitochondrial DNA repair. The bioenergetics defect in AOA1-mutant fibroblasts and APTX-depleted Hela cells is caused by decreased expression of SDHA and genes encoding CoQ biosynthetic enzymes, in association with reductions of APE1, NRF1 and NRF2. The biochemical and molecular abnormalities in APTXdepleted cells are recapitulated by knockdown of APE1 in Hela cells and are rescued by overexpression of NRF1/2. Importantly, pharmacological upregulation of NRF1 alone by 5-aminoimidazone-4-carboxamide ribonucleotide does not rescue the phenotype, which, in contrast, is reversed by the upregulation of NRF2 by rosiglitazone. Accordingly, we propose that the lack of aprataxin causes reduction of the pathway APE1/NRF1/NRF2 and their target genes. Our findings demonstrate a critical role of APTX in transcription regulation of mitochondrial function and the pathogenesis of AOA1 via a novel pathomechanistic pathway, which may be relevant to other neurodegenerative diseases.

## Introduction

Ataxia oculomotorapraxia type 1 (AOA1) is an autosomal recessive cerebellar disease characterized by early-onset cerebellar ataxia, oculomotor apraxia, absence of tendon reflexes, distal loss of sense of position and vibration, and pyramidal weakness of the legs and peripheral neuropathy, often associated with hypoalbuminemia, hypercholesterolemia and mental retardation (1–6).

AOA1 is caused by mutations in APTX, which encodes the DNA strand-break repair protein aprataxin (APTX) (7,8). Cell lines derived from AOA1 patients show enhanced sensitivity to a range of DNA damaging agents that generate single-strand breaks (SSBs) such as hydrogen peroxide (9), indicating a role for APTX in the cellular response to DNA damage and oxidative stress. The hypersensitivity to agents inducing oxidative DNA damage may be attributed to interactions of APTX with proteins involved in cellular response to oxidative damage (10). However, unlike Ataxia-Telangiectasia (A-T), A-T–like disorders, xeroderma pigmentosum or other autosomal recessive cerebellar ataxias caused by DNA repair or maintenance defects, AOA1 patients do not manifest immunodeficiency or cancer susceptibility (11). Furthermore, assessments of DNA strand-break repair in AOA1 human fibroblasts and different APTX$^{-/-}$ mouse cell lines have produced conflicting results (9,12–15), suggesting that factors other than nuclear DNA damage may be involved in the pathogenesis of this disease.

Aprataxin also is thought to regulate transcription via RNA binding (16), interactions with RNA binding proteins, nucleolar distribution and delocalization after transcription inhibition (17). Nevertheless, despite manifesting significant decrease in nucleolar staining of nucleolin, fibroblasts carrying the common APTX W279X mutation did not show defects in rRNA transcription (17).

Interestingly, in muscle and/or fibroblasts of patients with AOA1 carrying the stop-codon mutation p.W279X, we and other investigators have observed decreased levels of coenzyme $Q_{10}$ (ubiquinone, $CoQ_{10}$), an antioxidant and electrons transporter, which carries electrons from Complexes I (NADH dehydrogenase) and II [succinate dehydrogenase (SDH)] to Complex III

(cytochrome bc1 complex) of the mitochondrial respiratory chain (5,18–20). In AOA1 patients, supplementation with $CoQ_{10}$ was associated with increased strength and energy level and disappearance of seizures in the affected individuals (18,21), suggesting a role of $CoQ_{10}$ deficiency in the pathogenesis of AOA1.

Recently, the role of aprataxin in the maintenance of mitochondrial DNA (mtDNA) has been investigated. Sykora and colleagues showed that APTX also localizes to mitochondria and that depletion of APTX in human SH-SY5Y neuroblastoma cells and primary skeletal muscle myoblasts results in reduced activity of citrate synthase (CS) (an index of mitochondrial mass), mtDNA damage and decreased mtDNA copy number (22).

However, the mechanisms underlying $CoQ_{10}$ deficiency secondary to APTX mutations remain elusive. In this work, we show that mitochondrial dysfunction, including $CoQ_{10}$ deficiency, in W279X-mutant fibroblasts from AOA1 patients and APTX-depleted Hela cells is independent of APTX role in nuclear or mtDNA repair and is mediated by downregulation of genes encoding mitochondrial proteins, including enzymes involved in $CoQ_{10}$ biosynthesis, via APE1, NRF1 and NRF2.

## Results

### APTX-mutant fibroblasts show reduced levels and biosynthesis of CoQ10.

We previously reported low levels of $CoQ_{10}$ in three AOA1 fibroblasts (P1, P2 and P3) (18). Therefore, we measured $CoQ_{10}$ levels in six additional fibroblasts cell lines carrying different APTX mutations. In total, five homozygous p.W279X-mutant cell lines (P1, P2, P5, P7 and P9) and two compound heterozygous (p.W279X/p.Q181X; p.W279X/unknown mutation) cell lines (P8
and P3) showed decreased levels of $CoQ_{10}$ (Table 1). One cell line, homozygous for the common mutation p.W279X (P6), and one cell line harboring another homozygous stop-codon mutation (p.R306X/p.R306X) (P4) showed normal levels of $CoQ_{10}$ (Table 1).

To define the cause of $CoQ_{10}$ deficiency, we studied the biosynthesis of $CoQ_{10}$ in the seven cell lines with reduced $CoQ_{10}$ levels, using two different assays. First, using $^{14}$C-PHB as a substrate, we analyzed the activity of the condensation of parahydroxybenzoate (PHB) and decaprenyl diphosphate (DPP). AOA1 patients' fibroblasts incubated with 14C-PHB showed 60% CoQ10 synthesis relative to control cells (Table 1). Although all cell lines with CoQ10 deficiency show decreased CoQ10 biosynthesis, the degree of CoQ10 deficiency in individual patients does not correlate with the severity of impairment of CoQ10 biosynthesis. There is a correlation between the mean CoQ10 level and mean CoQ10 biosynthesis activity (Table 1).

In the second assay, homogenates from three patient (P1–P3) and control fibroblasts incubated with 3H-DPP revealed normal CoQ10 synthesis in the patients' cells compared with controls (Table 1). The isoprenoid side chain DPP is produced by addition of isopentenyl diphosphate (IPP) molecules to farnesyl diphosphate (FPP) or geranylgeranyl diphosphate (GPP) through multiple steps, ultimately catalyzed by DPP synthase. The deficit of CoQ10 synthesis detected only in the first assay indicates decreased DPP synthase activity and normal activities of downstream enzymes.

### APTX-mutant fibroblasts show reduced succinate dehydrogenase

To address whether CoQ10 deficiency was associated with other mitochondrial abnormalities, we assessed respiratory chain enzymes activities and mitochondrial mass in patients' fibroblasts with decreased levels of CoQ10.

As CoQ10 transfers electrons from Complexes I and II to Complex III, we measured Complex I + III and II + III activities, and we observed mild decrease in Complex I + III activities (61 ± 7% of controls) (Fig. 1A), consistent with the mild CoQ10 deficiency, and normal Complex II + III activities (controls: 100 ± 9%, patients: 100 ± 10%). In contrast, SDH (Complex II) activity was significantly reduced (63 ± 9% of controls, Fig. 1B), and SDH protein levels were reduced, although not significantly (71 ± 9% of controls, Fig. 2A).

CS activity (89 ± 9% of controls, Fig. 1C) and TOM20 levels (controls: 100 ± 9%, patients: 86 ± 12%), two indices of mitochondrial mass and mtDNA copy number (controls: 100 ± 9%, patients: 105 ± 12%) were comparable in mutant and control fibroblasts. Therefore, the low levels of CoQ10, Complex I + III activity and Complex II in APTX-mutant fibroblasts are not caused by reduced mitochondrial content.

### APTX-mutant fibroblasts manifest reduced cell respiratory control ratio

In order to assess the metabolic consequences of the mitochondrial abnormalities observed, we assessed the energy metabolism in CoQ10-deficient fibroblasts. Adenosine triphosphate (ATP) turnover, expressed as coupling efficiency, showed no differences between control and APTX-mutant fibroblasts. However, respiratory control ratio was reduced in AOA1 cells with decreased CoQ10 and Complex II (62 ± 19% of controls) relative to controls (Fig. 1D). In contrast, an AOA1 cell line with normal CoQ10 and Complex II (P4) behaved as controls. The diminished cell respiratory control ratio reflects defective electron transport through the respiratory chain Complexes I–IV and may be caused by both decreased CoQ10, which shuttles electrons between
Complexes I and II to III, and low Complex II activity.

## Aprataxin knockdown in Hela cells recapitulates the phenotype of AOA1-mutant fibroblasts

To further investigate the function of APTX, we used shRNAmediated knockdown in Hela cells. The sequence of the selected shRNA (TRCN0000083642) interfered expression of nuclear and mitochondrial aprataxin isoforms. Clones with <20% of wildtype levels of APTX transcript (17 ± 5% of controls) and protein (24 ± 5% of controls) were chosen to verify the effects of lack of APTX.

Aprataxin-depleted Hela cells did not show growth defects or changes in morphology. The levels of CoQ10 were significantly decreased in the APTX-interfered clones compared with those expressing only scramble shRNA (shScramble: 100 ± 11%; shAPTX 71 ± 8%). Consistently, Complex I + III activities were mildly decreased in APTX knockdown cells (81 ± 12% of controls) compared with control cell lines (Fig. 1F), and Complex II + III activity was comparable in knockdown and control cell lines (shScramble: 100 ± 14%, shAPTX: 105 ± 12%).

As in mutant fibroblasts, SDH (Complex II) activity and protein level were reduced in APTX-depleted cells (64 ± 9 and 75 ± 4% of controls) (Figs 1G and 2B), and CS activity was normal (Fig. 1H). Surprisingly, significant increase in mtDNA levels (shScramble: 100 ± 9, shAPTX: 120 ± 4%) and in TOM20 protein levels (shScramble: 100 ± 9, shAPTX: 138 ± 11%) were observed.

## APTX-mutant fibroblasts and APTX-depleted cells show reduced mRNA expression and protein levels of PDSS1, the first committed enzyme of CoQ10 biosynthesis

As the radioactive biosynthetic assays in APTX-mutant fibroblasts with low CoQ10 indicated a defect in CoQ10 biosynthesis, we investigated the steps of CoQ10 biosynthesis in the CoQ10-deficient cell lines, by measuring mRNA and protein levels of the 12 known enzymes known to be involved in the CoQ10synthetic pathway and/or its regulation.

Fibroblasts with the p.W279Xmutation and low levels of CoQ10 showed significantly reduced expression of PDSS1 (60 ± 6% of controls), a subunit of the first committed enzyme of the CoQ10 biosynthetic pathway (Fig. 3A), consistent with the reduction in CoQ10 levels and biosynthesis observed in the same cell lines. In contrast, P4 and P6, which had normal levels of CoQ10, had normal PDSS1 mRNA levels (P4 = 115 ± 20% and P6 = 124 ± 17% of controls) and normal or increased mRNA levels of the other enzymes of the pathway (Supplementary Material, Fig. S1).

Reduced PDSS1 mRNA expression in patient fibroblasts correlated with decreased PDSS1 protein levels (40 ± 5% of controls) (Fig. 3B). PDSS1 mRNA and protein levels were also significantly decreased in APTX-depleted Hela cells, compared with wildtype cells (73 ± 6 and 64 ± 4% of controls) (Fig. 3C and D). The decrease of PDSS1, the first committed enzyme of CoQ10 biosynthetic pathway, which catalyzes elongation of GPP or FPP with several IPP groups to form the decaprenyl chain, accounts for the reduced incorporation of 14C-PHB into AOA1 cells.

To exclude the possibility of PDSS1 mutations causing reduction in mRNA and encoded protein, we sequenced exons and flanking intronic regions of PDSS1 in one AOA1 patient (P3) and did not find any alterations.

## Levels of APE1 are reduced in APTX-mutant and APTX-depleted cells

Because APTX interacts with a variety of proteins through the forkhead-associated (FHA) domain, we initially excluded a direct interaction between APTX and PDSS1 protein by

co-immunoprecipitation. Then, we analyzed the levels of APE1 and PARP-1, two interacting partners of aprataxin involved in mitochondrial function (23–25).

AOA1 fibroblasts with CoQ10 deficiency showed decreased levels of APE1 (77 ± 5% of controls) (Fig. 4A), and not statistically significant decrease of PARP-1 (controls: 100 ± 11, patients: 68 ± 5% of controls), whereas AOA1 cells with normal CoQ10 levels (P4 and P6) had normal amounts of APE1 and PARP1 (P4: APE1 106 ± 5% and PARP-1 103 ± 2%; P6: APE1 119 ± 28% and PARP-1 99.8 ± 14% of controls). In APTX-depleted Hela cells, only APE1 was reduced (67 ± 11% of controls) (Fig. 4D), whereas PARP1 remained unaltered (shScramble: 100 ± 9%, shAPTX: 102 ± 10%). Therefore, decreased APE1 level is a shared feature of W279Xmutant and APTX knockdown cells with low CoQ10, suggesting a role of this protein in the pathogenesis of mitochondrial abnormalities in APTX-mutant and APTX-depleted cells.

## Nuclear respiratory factors 1 and 2 are reduced in APTX-mutant and APTX-depleted cells

Multiple mitochondrial genes, including succinate dehydrogenase subunit A (SDHA), are co-regulated by NRF1 and NRF2 (26,27), and published studies have shown that mitochondrial
genes are downregulated in APE1-deficient cells (23,28) owing to the regulatory role of APE1 on DNA-binding and transcriptional activity of NRF1. Therefore, we assessed steady-state levels of
NRF1, and NRF2, in AOA1 fibroblasts and APTX-depleted cells. Only the fibroblasts with at least one copy of the p.W279X mutation and APTX knockdown cells, which had low levels of CoQ10
and APE1, showed decreased steady-state levels of both transcription factors (NRF1:67 ± 7%, NRF2:70 ± 3% of controls) (Fig. 4B and C), consistent with the mild reduction of CoQ10 and SDHA protein in these cells. In contrast, AOA1 fibroblasts without deficiency of CoQ10 or complex II showed normal levels of NRF1 and NRF2 (P4: NRF1 103 ± 2% and NRF2 118 ± 13%; P6: NRF1 91 ± 22% and NRF2 84 ± 15% of controls).

We analyzed also the levels of PGC1α, a positive regulator of mitochondrial biogenesis and respiration (29), which contributes to the detoxification of reactive oxygen species (ROS) and regulates NRF1 and NRF2 (30–32). No reduction was observed in PGC1α protein in AOA1 cells (100 ± 24% of controls) or in APTXdepleted clones (93 ± 12% of controls), thereby we excluded
reduction of PGC1α as the cause of the diminished levels of NRF1 and NRF2.

Of relevance, several NRF2-binding sites are located within the vicinity of PDSS1 (chr10:26 963 258–27 012 389) (26 985 881–26 987 419, 27 149 588–27 150 373, 27 147 561–27 147 820, 26 981 519–26 981 778; HGMD® Human Gene Mutation Database), which showed decreased expression in AOA1 and APTX-depleted cells. These findings suggest that NRF2, which is reduced in APTX-depleted cells, regulates PDSS1 expression. In addition, NRF2-binding sites reside in close association with other CoQ10 biosynthetic enzyme genes as PDSS2 (chr6:107 473 761–107 780 779) (107 780 508–107 781 486) and COQ5 (chr12:120 941 082–120 966 964) (120 966 550–120 967 201, 120 971 948–120 972 435, 120 967 121–120 967 375, 120 972 230–120 972 474) (HGMD® Human Gene Mutation Database), which were downregulated in APTX knockdown cells (Fig. 5).

## APE1 depletion impairs NRF1 expression in Hela cells and resembles APTX knockdown clones

To confirm the role of the lack of APE1 in the pathogenesis of mitochondrial abnormalities in APTX-depleted cells via NRF1/NRF2, we knocked down APE1. ShRNA-mediated APE1 knockdown clones with 53 ± 11% of control protein levels showed lower levels of NRF1 transcript (43 ± 3% of controls) and protein (64 ± 10%) (Fig. 6). In addition, in those clones, we observed reduced expression of NRF2, PDSS1 and SDHA and protein levels (Fig. 6) similar to the reductions found in APTX-depleted cells (Figs 2B, 3D and 4F), confirming that the lack of APE1 decreases NRF1 leading to the mitochondrial biochemical and molecular defects observed in APTX-mutant cells.

## Overexpression of NRF1 increases PDSS1 and SDHA in APTX-depleted cells

To further validate the hypothesis that the reduction of NRF1, and, in turn, NRF2, causes mitochondrial respiratory impairment in APTX-depleted clones, we overexpressed NRF1 in APTXdepleted Hela cells. Different clones expressing high levels of NRF1 transcript and protein levels (Fig. 7A and B) were assessed to determine effects on the expression of PDSS1, SDHA and COQ5 transcripts, and their protein levels (Fig. 7C and D). In addition, we measured the levels of NRF2 and TOM20 (Fig. 7D). Stable transfection of NRF1 restored the normal level of NRF1 protein in APTX-depleted clones (Fig. 7B). In contrast, NRF1 protein levels did not increase when NRF1 construct was expressed in control cells, suggesting a tight normal physiological regulation of NRF1 protein levels.

Increased expression of NRF1 raised the levels of NRF2 protein in APTX knockdown cells, returning its value to levels comparable with control clones (Fig. 7D). Also PDSS1, SHDA and COQ5 protein levels were increased in APTX-depleted clones expressing NRF1 compared with APTX-depleted clones with empty vectors (Fig. 7D). Overexpression of NRF1 also increased the levels of CoQ10 in the clones expressing NRF1 compared with controls (shScramble-EV: 100 ± 14%, shAPTX-EV: 81 ± 7%, shScramble-NRF1: 127 ± 26% and shAPTX-NRF1: 365 ± 103%). We did not observe an increase of TOM20 (Fig. 7D) or mtDNA in NRF1-expressing clones (shScramble-NRF1: 99 ± 3%, shAPTX-NRF1: 98 ± 2%). Thus, the upregulation of NRF2 mediated by overexpression of NRF1 complemented the molecular alterations observed in APTX-depleted Hela cells, indicating that deficiencies of both NRFs contribute to mitochondrial dysfunction in AOA1.

## Rosiglitazone increases the expression of PDSS1 in AOA1 fibroblasts through NRF2

5-aminoimidazone-4-carboxamide ribonucleotide (AICAR) and rosiglitazone are two commercially available compounds, which have been shown to affect mitochondrial biogenesis and function through the upregulation of NRF1 and NRF2 (33). Therefore, we treated AOA1 fibroblasts with these pharmaceutical agents to assess their impact on NRFs levels and downstream effects.

AICAR significantly increased NRF1 protein levels in AOA1-mutant fibroblasts (Fig. 8A), but did not elevate PDSS1 levels. In contrast, rosiglitazone increased the levels of NRF2 and PDSS1 significantly (Fig. 8B). SDHA and TOM20, two NRF1-targeted genes, showed trends toward increases after both treatment (Fig. 8A). These results support the role of NRF2 in the transcriptional regulation of PDSS1 gene.

## Discussion

We and other investigators have observed CoQ10 deficiency secondary to mutations in aprataxin (5,18–20), a nuclear DNA-processing protein that hydrolyses 5′-adenylated DNA (12,34,35), and, when mutated, causes the neurodegenerative disease AOA1. Although aprataxin predominantly resides in nuclei (9,10,14,36), in neural-like cells, it has also been localized to mitochondria where it has been shown to preserve mitochondrial function and to prevent accumulation of mtDNA damage (22).

Here, we have observed that CoQ10 deficiency in APTX-mutant and APTX-depleted cells is due to diminished CoQ10 biosynthesis, and it is associated with reduced respiratory capacity, decreased mitochondrial respiratory chain enzymes and normal mtDNA content, suggesting that, despite the putative role of aprataxin in maintaining mtDNA integrity, mitochondrial dysfunction in APTX-depleted cells is not due to its involvement in mtDNA repair but rather is related to its role in transcription regulation, and consequent impairment of the APE1/NRFs pathway, which plays a critical role in the cross-talk between nucleus and mitochondria.

APE1, a binding partner of APTX, has been described as a dualfunction protein involved in base excision repair (BER), and in eukaryotic transcriptional regulation of gene expression (37), probably as consequence of the redox co-activation of various transcription factors including NRF1 (23), a regulator of mitochondrial function and biogenesis (26). It has been reported that decreased APE1 levels are associated with reduced NRF1 DNA-binding activity and consequent altered expression of downstream genes (23). In this study, we show that APTX deficiency causes depletion of APE1 and leads to reduction of NRF1, which in turns downregulates NRF2, and the downstream targets SDHA and PDSS1, causing deficiencies of SDH and CoQ10. NRF2- binding sites regulate SHDA expression (38) and have been found in close proximity to PDSS1. Moreover, NRF2 target sequences are also present in other genes, such as PDSS2 and COQ5, which are reduced in APTX-depleted cells. Thus, we hypothesize

that the mitochondrial alterations linked to downregulation of APE1 and NRF1 are mediated by the reduction of NRF2.

This hypothesis is supported by the observation that the upregulation of NRF2 mediated by NRF1 overexpression ameliorates molecular and biochemical abnormalities in APTX-depleted cells, and treatment with rosiglitazone, an anti-diabetic drug, which increases NRF2 transcript, rescues the abnormal biochemical phenotype in AOA1 fibroblasts. In contrast, AICAR, which enhances NRF1 expression (33), does not ameliorate the mitochondrial defects in the APTX-mutant cells. The activation of NRF1 by AICAR is not a specific effect, because AICAR, through activation of AMPK (39), acts on several other transcription factors, co-activators and co-repressors. This may explain why pharmacological upregulation of NRF1 through AICAR does not cause NRF2 upregulation, which we have observed after NRF1 overexpression. We have also excluded the possibility that the rescue is due to increased mitochondrial biogenesis, because multiple indeces of mitochondrial mass are unaltered after NRF1 overexpression.

We believe that APE1 plays a key role in regulating CoQ biosynthesis through PDSS1 and COQ5 in W278X-mutant and APTX-depleted cells, because APE1, PDSS1 and COQ5 levels are reduced in W279X-mutant cells with reduced CoQ10; moreover, we found that P4 (homozygote R306X mutant) has normal levels of transcripts for biosynthetic genes, APE1 and NRFs. In contrast, P6 (homozygote W279X with normal CoQ10 level) showed increased expression of all the biosynthetic genes, except PDSS1 and COQ5, and normal APE1 levels.

The bioenergetic defect observed in AOA1 could be caused by CoQ10 deficiency, and consequent reduction in Complex I + III activities, or by SDH deficiency, which, although caused by different mechanism, is also a feature of Friedreich ataxia, another autosomal recessive ataxia (40). Although we cannot account for the normal levels of Complex II + III activities, some studies indicate that CoQ is compartmentalized into two intracellular CoQ pools, one of which transfers electrons from the CI oxidation of the NADH to CIII (CoQNAD) and the other one transfers electrons from the CII oxidation of the FADH2 to CIII (CoQFAD). CI, but not CII, physically interacts with CIII in the formation of supercomplexes, which contain the CoQNAD pool, whereas CIII molecules that are free of interaction with CI are mainly responsible for CoQFAD oxidization (41). Thus, if CoQ10 deficiency in AOA1 decreases CIII bound to CI (supercomplex) (42), increased free CIII will be available for CII and may be reflected by a normalization of the CII + III activity.

Although SDH and CoQ10 deficiency were observed in both AOA1 fibroblasts and APTX-depleted Hela cells, only CS activity was slightly decreased in AOA1 fibroblasts, whereas the levels of mtDNA and TOM20 were significantly increased in APTX-depleted cells. The differences in these indices of mitochondrial mass between AOA1-mutant and APTX-depleted cells suggest cell type-specific stress response or compensatory mechanisms. CS has been noted to be reduced in APTX-depleted neuroblastoma cells (22), possibly due to loss of dysfunctional mitochondria. The mild biochemical defects in mitochondrial respiratory chain activities, CoQ10 level and oxidative phosphorylation observed in AOA1 fibroblasts may reflect more severe abnormalities in other tissues, as tissue specificity is frequently observed in mitochondrial disorders including the autosomal recessive cerebellar ataxia caused by ADCK3 mutations, the most common primary CoQ10 deficiency (43). ADCK3 is an atypical protein kinase that regulated CoQ biosynthesis and is the homolog of coq8 in yeast (44). Previous studies of ADCK3-mutant fibroblasts demonstrated mild CoQ10 deficiency and mitochondrial respiratory chain defects strikingly similar to those observed in APTXmutant cells, and have slightly increased ROS production and proteins and lipid oxidation when stressed with glucose-free medium (45). Moreover, in some patients carrying ADCK3 mutations, CoQ10 deficiency is limited to muscle and does not extend to fibroblasts further indicating tissue-specific effects (43). However, the lack of studies of the cerebellum has precluded empirical testing of the hypothesized neuron-specific defects. Alternatively, the mild biochemical defects may be sufficient to damage vulnerable cells in the cerebellum in this chronic and slowly progressive disease.

While our observations that the mitochondrial dysfunctions in AOA1 fibroblasts are related to the instability of APE1 and the consequent reduction of NRF1 and NRF2 are important, further studies are necessary to address the mechanisms of interaction and stabilization of APE1 by APTX and to understand the role of other factors, such as potential genetic modifiers causing phenotype variability, in order to explain why not all AOA1 cells

carrying the p.W279X mutation show mitochondrial impairment, because it has been previously shown that mutant APTX becomes unstable regardless of the mutation (9,14,46).

Interestingly, in other neurodegenerative disorders caused by defects in proteins involved in DNA break repair, impairments of other nuclear-mitochondrial cross-talk pathways have been observed. Fang et al. reported hyper-activation of PARP-1, which causes NAD + -SIRT1-PGC-1α-UCP2 axis depression, and in turn, defective mitophagy (25). However, we did not observe abnormal levels of PARP-1 and PGC1-α in APTX-mutant/depleted cells; therefore, we have excluded involvement of this pathway in AOA1. Defects in this or other pathways leading to downregulation of transcription factors involved in respiratory gene expression may account for secondary mitochondrial dysfunctions in other diseases. For example, mice lacking Hint2, a mitochondrial protein belonging to the histidine triad (HIT) superfamily to which aprataxin belongs, manifest accelerated hepatic steatosis, mitochondrial abnormalities, including CoQ10 deficiency, and downregulation of genes encoding proteins involved in mitochondrial fusion and fission (47). Defective CoQ biosynthesis has been found also in cells lacking mitofusin 2 (MNF2), associated with Charcot Marie Tooth type 2A disease (29).

The mitochondrial abnormalities we observed in APTX-mutant and APTX-depleted cells may be downstream effects in response to genotoxic stress, because elevated levels of 8-oxo-dG and hypersensitivity to agent causing DNA SSBs have been observed in AOA1- mutant fibroblasts (9,10,13). In summary, our findings shed some light on the link between APTX and mitochondrial function, which may lead to better understanding of the pathogenesis ofAOA1 and other degenerative disorders. Uncovering the contribution of altered nuclear-mitochondrial cross-talk pathways to mitochondrial dysfunction is important to identify targets for novel therapeutic approaches.

## Materials and Methods

### Cells culture and pharmacological treatment

All experiments were performed in human skin fibroblasts from at least three controls and six AOA1 patients (Table 1), unless differently specified. Skin fibroblasts and Hela cells were grown in Dulbecco's modified Eagle medium (DMEM) supplemented with 10% fetal bovine serum (FBS), 5 ml MEM non-essential amino acids, 5 ml of MEM vitamin solution and 5 ml of penicillin–streptomycin (total volume 565 ml) until confluence. Cells were grown to perform each experiment in replicates. AOA1 fibroblast cells were treated for 72 h either with 60 μM of rosiglitazone (ICS International Clinical Service GmbH, S2505; dissolved in DMSO) or 0.5 mM of AICAR (Toronto Research Chemicals, A611700; dissolved in water) (33) or with the respective vehicle in regular medium. After the treatment, cells were collected and analyzed.

### CoQ10 level measurement

To measure CoQ10, cells were grown in 15-cm-diameter culture plates until confluence. CoQ10 was extracted in a hexane:ethanol mixture (48). The lipid component of the extract was separated by high-performance liquid chromatography (HPLC) on a reverse Symmetry® C18 3.5 μm, 4.6 × 150 mm column (Waters), using a mobile phase consisting of methanol, ethanol, 2-propanol, acetic acid (500:470:15:15) and 50 mM sodium acetate at a flow rate of 0.8 ml/min. The electrochemical detector consisted of an ESACoulochemII with the following setting: guard cell (upstreamof the injector) at +900 mV, conditioning cell at −650 mV (downstream of the column), followed by the analytical cell at +450 mV. CoQ10 concentration was estimated by comparison of the peak area with those of standard solutions of known concentration, and the results were normalized to mg protein.

### CoQ10 biosynthesis assays

We performed biochemical assays to measure incorporation of two radiolabeled substrates (49). For the first assay, AOA1 and control fibroblasts were plated in six-well plates (40 000 cells/ well) and were cultured using DMEM with 10% fetal calf serum. After 2 days, the medium was replaced by fresh DMEM with 0.1 μCi of 14C-PHB (50 Ci/mol specific activity). After incubation for additional 24 h, cells were washed twice with phosphate-buffered saline (PBS) and collected by using 0.5 ml of 1% sodium dodecyl sulfate (SDS), followed by shaking for 10 min at room temperature (twice). The contents of each plate were combined (3 ml total), and 0.2 ml was saved for protein determination. The remaining pooled suspensions were subjected to hexane extraction. CoQ10 was extracted adding 4ml hexane–ethanol (5/2 v/v) and vortexing for 2 min. After centrifugation at 2500 rpm at room temperature for 5 min, the upper phase was carefully transferred into a 20-ml glass scintillation vial. The combined extract was evaporated

under a gentle stream of N2 gas, and the residue was dissolved in 0.15 ml of 1-propanol. Fifty microliters of the extract was directly injected into the HPLC. The waste line of HPLC was connected to a fraction collector, programed to collect 1.0 ml of fractions per minute. CoQ10 peak was identified by specific retention time determined after injection of a known amount of authentic CoQ10. The amount of radioactivity in the collected fraction was determined in a Packard scintillation counter. In the second assay, the incubation mixture contained 250 nCi of 3H-radiolabeled decaprenyl pyrophosphate (decaprenyl-PP) (20 Ci/mmol) solubilized in 25 µl of 1% Triton X-100, 50 mM potassium phosphate, pH 7.5, 10 mM MgCl2, 5mM ATP, 20 µM 4-hydroxybenzoic acid and fibroblast lysate (1 mg protein) in a total volume of 0.5 ml. After incubation at 37°C in a shaking water bath for 60 min, the reaction was stopped by adding 1 ml of ethanol, followed by 1 ml of 0.1 M SDS. Hexane extraction was carried out as mentioned earlier, and the residue was dissolved in 100 µl of 1-propanol. An aliquot of 50 µl was injected into the HPLC. Fraction collection and radioactivity measurement were performed as described earlier.

## Mitochondrial respiratory chain enzymes activity

The activity of mitochondrial respiratory chain enzymes was assessed spectrophotometrically (50). NADHcytochrome c reductase (NCCR) activity (Complex I + III)was measured by monitoring the rate of reduced cytochrome c formation using NADH as substrate. Changes in absorbance at 550 nm were monitored at 30°C over 1 min, followed by the addition of 10 µ rotenone and additional monitoring of absorbance for 2 min. Reduction of cytochrome c was determined based on the difference between the rate of absorbance change before and after rotenone was added. Succinate cytochrome c reductase (SCCR) activity (Complex II + III) was measured by monitoring the rate of reduced cytochrome c formation using succinate as substrate. Changes in absorbance were monitored at 30°C for 2 min at 550 nm. SDH (CII) activity was measured following reduction of 2,6-dichlorophenol- indophenol (DCIP) at 600 nm for 1 min. CS activity was measured following the reduction of 1m 5,5′-dithiobis (2-nitrobenzoic acid) at 412 nm (30°C) for 2 min. Enzymes activities were normalized to proteins.

## OCR and ECAR measurements

Oxygen consumption rate (OCR) and extracellular acidification rate (ECAR) in AOA1 and control fibroblasts were measured with an XF24 Extracellular Flux Analyzer (Seahorse Bioscience, Billerica, MA, USA). Coupling efficiency was assessed by the reduction in oxygen consumption after oligomycin injection, as the fraction of basal mitochondrial oxygen consumption used for ATP synthesis. Cell respiratory control ratio is the ratio of the uncoupled OCR [after addition of carbonyl cyanide 4-(trifluoromethoxy)phenylhydrazone (FCCP)] to OCR in the presence of oligomycin. Because it is the ratio of two rates, this parameter, as well as coupling efficiency, is sensitive to the sites of dysfunction and therefore is internally normalized (51). Each cell line was seeded in five wells of an XF 24-well cell culture microplate (Seahorse Bioscience) at a density of 60 000 cells/well. Forty minutes before the assay, growth medium was replaced with 525 µl of bicarbonate- free DMEM pre-warmed at 37°C. After baseline measurements of OCR (OCR-B), OCR was measured after sequentially injection to each well of 75 µl of oligomycin (OL), 75 µl of FCCP and 75 µl of rotenone and antimycin A, to reach working concentrations of 1, 0.75, 1 and 1 µM, respectively. Non-mitochondrial respiration was subtracted from all the rates before analysis.

## COQ gene expression by real-time PCR

Quantitative real-time reverse transcriptase-polymerase chain reaction (RT–PCR) was performed to measure the expression of genes required for CoQ10 biosynthesis (COQ genes). Total RNA was extracted fromcells using PureLinkTM RNA Mini Kit (Ambion) according to the manufacturer''s instructions. Purified total RNA (100 ng) was reverse-transcribed to cDNA with SuperScript® VILO™ cDNA Synthesis Kit (Invitrogen) after digestion with DNase I (Roche). Quantitative RT–PCR was performed using TaqMan® Assays for each gene (Applied Biosystems, Invitrogen). The expression of the target genes was calculated by delta-Ct method and normalized to the expression of β-actin.

## Immunoblotting analyses

Cell lysates were quantitated for total protein content using the Bradford system (ThermoScience) and analyzed by electrophoresis in an SDS 4–20% gradient polyacrylamide gel. After electrophoresis, proteins were transferred electrophoretically to polyvinylidene

difluoride membrane and probed with the following antibodies: anti-PDSS1 (3 μg/mL, Sigma), anti-APTX (1:1000, Abcam), anti-β-actin (1:50 000, Sigma), anti-vinculin (1:10 000,Sigma), anti-APE1 (1:1500, Abcam), anti-NRF1 (1:300, Santa Cruz), anti-NRF2 (1:500, Santa Cruz), anti-PARP1 (1:1500, BioRad), anti-SDHA (CII, 1:1000, Abcam), anti-TOM20 (1:1000, Santa Cruz) and anti-CoQ5 (1:200, Thermo Scientific). Peroxidase-conjugated anti-rabbit, anti-goat or anti-mouse IgG secondary antibodies (Santa Cruz Biotechnology) were used at a dilution of 1:2000, 1:10 000 and 1:5000, respectively. Protein bands were visualized by chemiluminescence, using reagents purchased fromGE Healthcare. Intensity of the bands was quantified with ImageJ.

## Generation of cells expressing shRNA/NRF1-overexpressing shAPTX cells

Hela cells were cultured in DMEM with 10% FBS until 70–80% confluent. Transfections with scramble shRNA-pLKO plasmid (used as control), APTX-specific TRC shRNA-pLKO plasmid construct (TRCN0000083642; Sigma), APE1-specific TRC shRNA-pLKO plasmid construct (TRCN00007958), ORF expression clone for NRF1 (BC016925.1) and empty control vector for pReceiver-M02 (used as control) were mediated by Lipofectamine 2000 (Invitrogen) according to the manufacturer's instructions. After 5 h of transfection, cells were selected with puromycin/neomycin in DMEM 2% FBS and transfected clones expanded separately with DMEM 10% FBS. Statistical analysis Statistical analyses were performed with GraphPad InStat. Shapiro– Wilk normality test was performed to assess the normality of the population distribution. Student's t-test or Mann–Whitney tests were used to assess significant differences. A P-value of $<0.05$ was considered to be statistically significant. Data were expressed as the mean ± SEM.


## Acknowledgements

The authors wish to express their gratitude to the participants of the 176th ENMC International Workshop: Diagnosis and Treatment of CoQ10 Deficiency, to Dr Michio Hirano and his laboratory's members for the insightful discussions, to Drs. Michio Hirano, Eric Schon and Serge Przedborski for critical reading of the manuscript. Conflict of Interest statement. None declared.

## Funding

This work has been supported by NIH P01 HD080642-01 (C.M.Q.). B.G.D. is supported by a grant from the 'Fundación Alfonso Martín Escudero', Spain; L.C.L. is supported by the 'Ramón y Cajal' National Programme, Ministerio de Economía y Competitividad, Spain (RYC-2011-07643); and C.M.Q. is supported also by NICHD 5K23 HD065871 and by the Muscle Dystrophy Association (MDA).


## References


1. Inoue, N., Izumi, K., Mawatari, S., Shida, K. and Kuroiwa, Y. (1971) Congenital ocular motor apraxia and cerebellar degeneration: report of two cases. Rinsho Shinkeigaku, 11, 855–861.

2. Uekawa, K., Yuasa, T., Kawasaki, S.,Makibuchi, T. and Ideta, T. (1992) A hereditary ataxia associated with hypoalbuminemia and hyperlipidemia—a variant form of Friedreich's disease or a new clinical entity? Rinsho Shinkeigaku, 32, 1067–1074.

3. Le Ber, I., Moreira, M.C., Rivaud-Pechoux, S., Chamayou, C., Ochsner, F., Kuntzer, T., Tardieu, M., Said, G., Habert, M.O., Demarquay, G. et al. (2003) Cerebellar ataxia with oculomotor apraxia type 1: clinical and genetic studies. Brain, 126, 2761–2772.

4. Tranchant, C., Fleury, M., Moreira, M.C., Koenig, M. and Warter, J.M. (2003) Phenotypic variability of aprataxin gene mutations. Neurology, 60, 868–870.

5. Castellotti, B., Mariotti, C., Rimoldi, M., Fancellu, R., Plumari, M., Caimi, S., Uziel, G., Nardocci, N., Moroni, I., Zorzi, G. et al. (2011) Ataxia with oculomotor apraxia type1 (AOA1): novel and recurrent aprataxin mutations, coenzyme Q10 analyses, and clinical findings in Italian patients. Neurogenetics, 12, 193–201.

6. Yokoseki, A., Ishihara, T., Koyama, A., Shiga, A., Yamada, M., Suzuki, C., Sekijima, Y., Maruta, K., Tsuchiya, M., Date, H. et al. (2011) Genotype-phenotype correlations in early onset ataxia with ocular motor apraxia and hypoalbuminaemia. Brain, 134, 1387–1399.

7. Moreira, M.C., Barbot, C., Tachi, N., Kozuka, N., Uchida, E., Gibson, T., Mendonca, P., Costa, M., Barros, J., Yanagisawa, T. et al. (2001) The gene mutated in ataxia-ocular apraxia 1 encodes the new HIT/Zn-finger protein aprataxin. Nat. Genet., 29, 189–193.

8. Date, H., Onodera, O., Tanaka, H., Iwabuchi, K., Uekawa, K., Igarashi, S., Koike, R., Hiroi, T., Yuasa, T., Awaya, Y. et al. (2001) Early-onset ataxia with ocular motor apraxia and hypoalbuminemia is caused by mutations in a new HIT superfamily gene. Nat. Genet., 29, 184–188.

9. Gueven, N., Becherel, O.J., Kijas, A.W., Chen, P., Howe, O., Rudolph, J.H., Gatti, R., Date, H., Onodera, O., Taucher-Scholz, G. et al. (2004) Aprataxin, a novel protein that protects against genotoxic stress. Hum. Mol. Genet., 13, 1081–1093.

10. Harris, J.L., Jakob, B., Taucher-Scholz, G., Dianov, G.L., Becherel, O.J. and Lavin, M.F. (2009) Aprataxin, poly-ADP ribose polymerase 1 (PARP-1) and apurinic endonuclease 1 (APE1) function together to protect the genome against oxidative damage. Hum. Mol. Genet., 18, 4102–4117.

11. Palau, F. and Espinos, C. (2006) Autosomal recessive cerebellar ataxias. Orphanet. J. Rare Dis., 1, 47.

12. Reynolds, J.J., El-Khamisy, S.F., Katyal, S., Clements, P., McKinnon, P.J. and Caldecott, K.W. (2009) Defective DNA ligation during short-patch single-strand break repair in ataxia oculomotor apraxia 1. Mol. Cell. Biol., 29, 1354–1362.

13. Mosesso, P., Piane, M., Palitti, F., Pepe, G., Penna, S. and Chessa, L. (2005) The novel human gene aprataxin is directly involved in DNA single-strand-break repair. Cell. Mol. Life Sci., 62, 485–491.

14. Hirano, M., Yamamoto, A., Mori, T., Lan, L., Iwamoto, T.A., Aoki, M., Shimada, K., Furiya, Y., Kariya, S., Asai, H. et al. (2007) DNA single-strand break repair is impaired in aprataxin-related ataxia. Ann. Neurol., 61, 162–174.

15. El-Khamisy, S.F., Katyal, S., Patel, P., Ju, L., McKinnon, P.J. and Caldecott, K.W. (2009) Synergistic decrease of DNA singlestrand break repair rates in mouse neural cells lacking both Tdp1 and aprataxin. DNA Repair (Amst), 8, 760–766.

16. Kijas, A.W., Harris, J.L., Harris, J.M. and Lavin, M.F. (2006) Aprataxin forms a discrete branch in the HIT (histidine triad) superfamily of proteins with both DNA/RNA binding and nucleotide hydrolase activities. J. Biol. Chem., 281, 13939–13948.

17. Becherel, O.J., Gueven, N., Birrell, G.W., Schreiber, V., Suraweera, A., Jakob, B., Taucher-Scholz, G. and Lavin, M.F. (2006) Nucleolar localization of aprataxin is dependent on interaction with nucleolin and on active ribosomalDNA transcription. Hum. Mol. Genet., 15, 2239–2249.

18. Quinzii, C.M., Kattah, A.G., Naini, A., Akman, H.O., Mootha, V. K., DiMauro, S. and Hirano, M. (2005) Coenzyme Q deficiency and cerebellar ataxia associated with an aprataxin mutation. Neurology, 64, 539–541.

19. Le Ber, I., Dubourg, O., Benoist, J.F., Jardel, C., Mochel, F., Koenig, M., Brice, A., Lombes, A. and Durr, A. (2007) Muscle coenzyme Q10 deficiencies in ataxia with oculomotor apraxia 1. Neurology, 68, 295–297.

20. D'Arrigo, S., Riva, D., Bulgheroni, S., Chiapparini, L., Castellotti, B., Gellera, C. and Pantaleoni, C. (2008) Ataxia with oculomotor apraxia type 1 (AOA1): clinical and neuropsychological features in 2 new patients and differential diagnosis. J. Child. Neurol., 23, 895–900.

21. Musumeci, O., Naini, A., Slonim, A.E., Skavin, N., Hadjigeorgiou, G.L., Krawiecki, N.,Weissman, B.M., Tsao, C.Y., Mendell, J.R., Shanske, S. et al. (2001) Familial cerebellar ataxia with muscle coenzyme Q10 deficiency. Neurology, 56, 849–855.

22. Sykora, P., Croteau, D.L., Bohr, V.A. and Wilson, D.M. 3rd. (2011) Aprataxin localizes to mitochondria and preserves mitochondrial function. Proc. Natl Acad. Sci. USA, 108, 7437–7442.

23. Li, M., Vascotto, C., Xu, S., Dai, N., Qing, Y., Zhong, Z., Tell, G. and Wang, D. (2012) Human AP endonuclease/redox factor APE1/ref-1 modulates mitochondrial function after oxidative stress by regulating the transcriptional activity of NRF1. Free Radic. Biol. Med., 53, 237–248.

24. Strosznajder, R.P., Czubowicz, K., Jesko, H. and Strosznajder, J. B. (2010) Poly(ADP-ribose) metabolism in brain and its role in ischemia pathology. Mol. Neurobiol., 41, 187–196.

25. Fang, E.F., Scheibye-Knudsen, M., Brace, L.E., Kassahun, H., SenGupta, T., Nilsen, H., Mitchell, J.R., Croteau, D.L. and Bohr, V.A. (2014) Defective mitophagy in XPA via PARP-1 hyperactivation and NAD(+)/SIRT1 reduction. Cell, 157, 882–896.

26. Scarpulla, R.C. (2002) Transcriptional activators and coactivators in the nuclear control of mitochondrial function inmammalian cells. Gene, 286, 81–89.

27. Scarpulla, R.C. (2008) Nuclear control of respiratory chain expression by nuclear respiratory factors and PGC-1-related coactivator. Ann. N Y Acad. Sci., 1147, 321–334.

28. Vascotto, C., Cesaratto, L., Zeef, L.A., Deganuto, M., D'Ambrosio, C., Scaloni, A., Romanello, M., Damante, G., Taglialatela, G., Delneri, D. et al. (2009) Genome-wide analysis and proteomic studies reveal APE1/Ref-1 multifunctional role in mammalian cells. Proteomics, 9, 1058–1074.

29. Mourier, A., Motori, E., Brandt, T., Lagouge, M., Atanassov, I., Galinier, A., Rappl, G., Brodesser, S., Hultenby, K., Dieterich, C. et al. (2015) Mitofusin 2 is required to maintain mitochondrial coenzyme Q levels. J. Cell Biol., 208, 429–442.

30. St-Pierre, J., Drori, S., Uldry, M., Silvaggi, J.M., Rhee, J., Jager, S., Handschin, C., Zheng, K., Lin, J., Yang,W. et al. (2006) Suppression of reactive oxygen species and neurodegeneration by the PGC-1 transcriptional coactivators. Cell, 127, 397–408.

31. St-Pierre, J., Lin, J., Krauss, S., Tarr, P.T., Yang, R., Newgard, C. B. and Spiegelman, B.M. (2003) Bioenergetic analysis of peroxisome proliferator-activated receptor gamma coactivators 1alpha and 1beta (PGC-1alpha and PGC-1beta) in muscle cells. J. Biol. Chem., 278, 26597–26603.

32. Valle, I., Alvarez-Barrientos, A., Arza, E., Lamas, S. and Monsalve, M. (2005) PGC-1 alpha regulates the mitochondrial antioxidant defense system in vascular endothelial cells. Cardiovasc. Res., 66, 562–573.

33. Hofer, A., Noe, N., Tischner, C., Kladt, N., Lellek, V., Schauss, A. andWenz, T. (2014) Defining the action spectrum of potential PGC-1alpha activators on a mitochondrial and cellular level in vivo. Hum. Mol. Genet., 23, 2400–2415.

34. Ahel, I., Rass, U., El-Khamisy, S.F., Katyal, S., Clements, P.M., McKinnon, P.J., Caldecott, K.W. andWest, S.C. (2006) The neurodegenerative disease protein aprataxin resolves abortive DNA ligation intermediates. Nature, 443, 713–716.
35. Rass, U., Ahel, I. andWest, S.C. (2007) Actions of aprataxin in multiple DNA repair pathways. J. Biol. Chem., 282, 9469–9474.

36. Clements, P.M., Breslin, C., Deeks, E.D., Byrd, P.J., Ju, L., Bieganowski, P., Brenner, C., Moreira, M.C., Taylor, A.M. and Caldecott, K.W. (2004) The ataxia-oculomotor apraxia 1 gene

product has a role distinct from ATM and interacts with the DNA strand break repair proteins XRCC1 and XRCC4. DNA Repair (Amst), 3, 1493–1502.

37. Li, M. and Wilson, D.M. 3rd. (2014) Human apurinic/apyrimidinic endonuclease 1. Antioxid. Redox Signal, 20, 678–707.

38. Piantadosi, C.A. and Suliman, H.B. (2008) Transcriptional regulation of SDHa flavoprotein by nuclear respiratory factor- 1 prevents pseudo-hypoxia in aerobic cardiac cells. J. Biol. Chem., 283, 10967–10977.

39. Merrill, G.F., Kurth, E.J., Hardie, D.G. andWinder,W.W. (1997) AICA riboside increases AMP-activated protein kinase, fatty acid oxidation, and glucose uptake in rat muscle. Am. J. Physiol., 273, E1107–E1112.

40. Puccio, H., Simon, D., Cossee, M., Criqui-Filipe, P., Tiziano, F., Melki, J., Hindelang, C., Matyas, R., Rustin, P. and Koenig, M. (2001) Mouse models for Friedreich ataxia exhibit cardiomyopathy, sensory nerve defect and Fe-S enzyme deficiency followed by intramitochondrial iron deposits. Nat. Genet., 27, 181–186.

41. Enriquez, J.A. and Lenaz, G. (2014) Coenzyme q and the respiratory chain: coenzyme q pool and mitochondrial supercomplexes. Mol. Syndromol., 5, 119–140.

42. Garcia-Corzo, L., Luna-Sanchez, M., Doerrier, C., Garcia, J.A., Guaras, A., Acin-Perez, R., Bullejos-Peregrin, J., Lopez, A., Escames, G., Enriquez, J.A. et al. (2013) Dysfunctional Coq9 protein causes predominant encephalomyopathy associated with CoQ deficiency. Hum. Mol. Genet., 22, 1233–1248.

43. Lagier-Tourenne, C., Tazir, M., Lopez, L.C., Quinzii, C.M., Assoum, M., Drouot, N., Busso, C.,Makri, S., Ali-Pacha, L., Benhassine, T. et al. (2008) ADCK3, an ancestral kinase, ismutated in a form of recessive ataxia associated with coenzyme Q10 deficiency. Am. J. Hum. Genet., 82, 661–672.

44. Gonzalez-Mariscal, I., Garcia-Teston, E., Padilla, S., Martin-Montalvo, A., Pomares-Viciana, T., Vazquez-Fonseca, L., Gandolfo- Dominguez, P. and Santos-Ocana, C. (2014) Regulation of coenzyme Q biosynthesis in yeast: a new complex in the block. IUBMB Life, 66, 63–70.

45. Quinzii, C.M., Lopez, L.C., Gilkerson, R.W., Dorado, B., Coku, J., Naini, A.B., Lagier-Tourenne, C., Schuelke, M., Salviati, L., Carrozzo, R. et al. (2010) Reactive oxygen species, oxidative stress, and cell death correlate with level of CoQ10 deficiency. FASEB J., 24, 3733–3743.

46. Sano, Y., Date,H., Igarashi, S., Onodera, O., Oyake, M., Takahashi, T., Hayashi, S., Morimatsu, M., Takahashi, H., Makifuchi, T. et al. (2004) Aprataxin, the causative protein for EAOH is a nuclear protein with a potential role as a DNA repair protein. Ann. Neurol., 55, 241–249.

47. Martin, J., Maurhofer, O., Bellance, N., Benard, G., Graber, F., Hahn, D., Galinier, A., Hora, C., Gupta, A., Ferrand, G. et al. (2013) Disruption of the histidine triad nucleotide-binding hint2 gene in mice affects glycemic control and mitochondrial function. Hepatology, 57, 2037–2048.

48. Lopez, L.C., Schuelke, M., Quinzii, C.M., Kanki, T., Rodenburg, R.J., Naini, A., Dimauro, S. and Hirano, M. (2006) Leigh syndrome with nephropathy and CoQ10 deficiency due to decaprenyl diphosphate synthase subunit 2 (PDSS2) mutations. Am. J. Hum. Genet., 79, 1125–1129.

49. Quinzii, C., Naini, A., Salviati, L., Trevisson, E., Navas, P., Dimauro, S. and Hirano, M. (2006) A mutation in parahydroxybenzoate-polyprenyl transferase (COQ2) causes primary coenzyme Q10 deficiency. Am. J. Hum. Genet., 78, 345–349.

50. Quinzii, C.M., Garone, C., Emmanuele, V., Tadesse, S., Krishna, S., Dorado, B. and Hirano, M. (2013) Tissue-specific oxidative stress and loss of mitochondria in CoQ-deficient Pdss2 mutant mice. FASEB J., 27, 612–621.

51. Brand, M.D. and Nicholls, D.G. (2011) Assessing mitochondrial dysfunction in cells. Biochem. J., 435, 297–312.

| Coenzyme $Q_{10}$ Patient | Mutation | CoQ (ng/mg prot) | CoQ (%) | CoQ biosynthesis (%) | References |
|---|---|---|---|---|---|
| P1 | pW279X/pW279X | 43.5 | 68.2 | 62.3 | (18) |
| P2 | pW279X/pW279X | 33.4 | 52.3 | 66.2 | (18) |
| P3 | pW279X/* | 46.4 | 72.7 | 54.5 | (18) |
| P4 | pR306X/pR306X | 95.1 | 149.0 | n/a | (5) |
| P5 | pW279X/pW279X | 27.7 | 43.4 | 39.7 | (5) |
| P6 | pW279X/pW279X | 61.9 | 97.0 | n/a | (5) |
| P7 | pW279X/pW279X | 40.4 | 63.3 | 45.3 | (5) |
| P8 | pW279X/pQ181X | 41.5 | 65.0 | 43.7 | (5) |
| P9 | pW279X/pW279X | 46.6 | 73.0 | 38.6 | (5) |
| Controls ($n = 8$) | | 63.8 ± 4.3 | 100 ± 6.8 | 100 ± 6.6 | |
| Biosynthesis of $CoQ_{10}$ | | | | | |
| Assay 1 | $CoQ_{10}$ synthesis | Percent of control mean | | | |
| Controls ($n = 7$) | 2945.4 ± 195 DPM/mg prot/day | 100 ± 6.6 | | | |
| Patients ($n = 7$) | 1796.3 ± 54 DPM/mg prot/day | 61.0 ± 1.8 | | | |
| Assay 2 | | | | | |
| Controls ($n = 5$) | 62.8 ± 10.4 DPM/mg prot/h | 100 ± 21.5 | | | |
| Patients ($n = 3$) | 56.4 ± 3.1 DPM/mg prot/h | 89.8 ± 4.9 | | | |

n/a, not available; DPM, disintegration per minute; prot, proteins.
Values are expressed as mean ± SEM.

Table 1. Coenzyme $Q_{10}$ levels in AOA1 skin fibroblasts and $CoQ_{10}$ biosynthesis using two radiolabeled substrates, $^{14}$C-PHB (50 Ci/mol) and $^{3}$H-decaprenyl-PP (20 Ci/mmol) in AOA1 skin fibroblasts

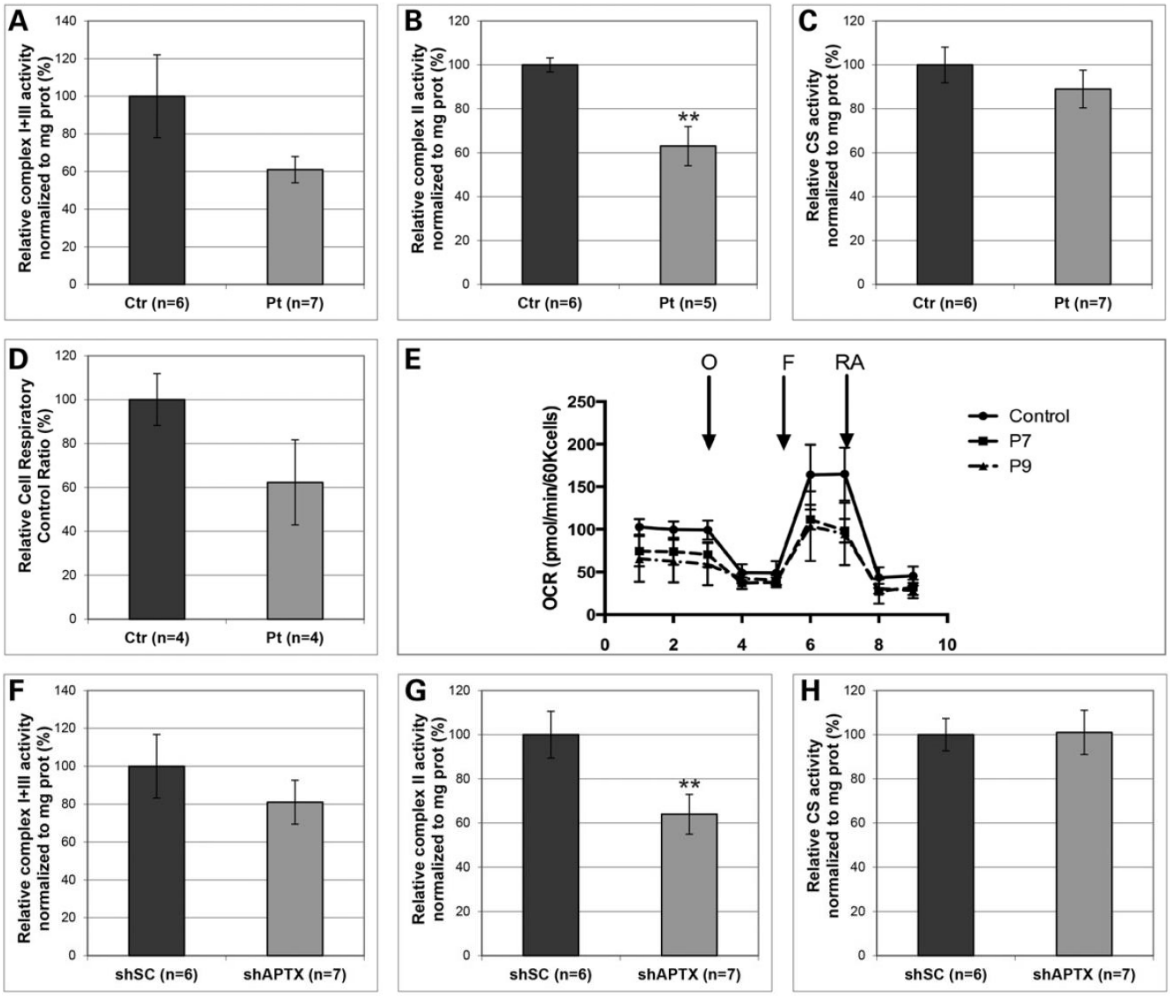


Figure 1. Mitochondrial respiratory function in APTX-mutant and APTX-depleted cells. Respiratory chain enzyme activities normalized to mg protein levels in AOA1 fibroblasts with CoQ10 deficiency (A–C) and in APTX-depleted Hela cells (F–H). Cell respiratory control ratio (D) of control and AOA1 fibroblasts. (E) Representative OCR of two control and two AOA1 cell lines. O, oligomycin; F, carbonyl cyanide-FCCP; RA, rotenone and antimycin. Data are expressed as mean ± SEM in relative percentage of controls (**P < 0.01).

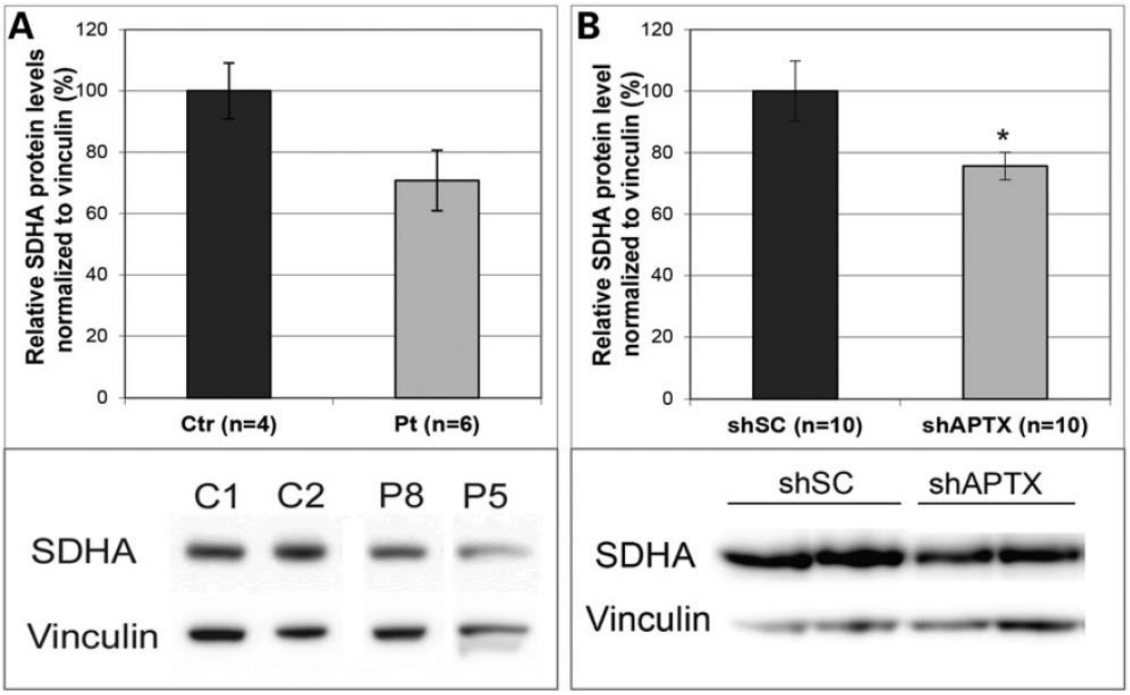


Figure 2. SDHA levels in APTX-mutant and APTX-depleted cells. Protein levels of SDHA are partially decreased in AOA1 fibroblasts with CoQ10 deficiency (A) and are significantly reduced in APTX-depleted cells (B). Representative western blot. Values are expressed as mean ± SEM in relative percentage of control (*$P < 0.05$).

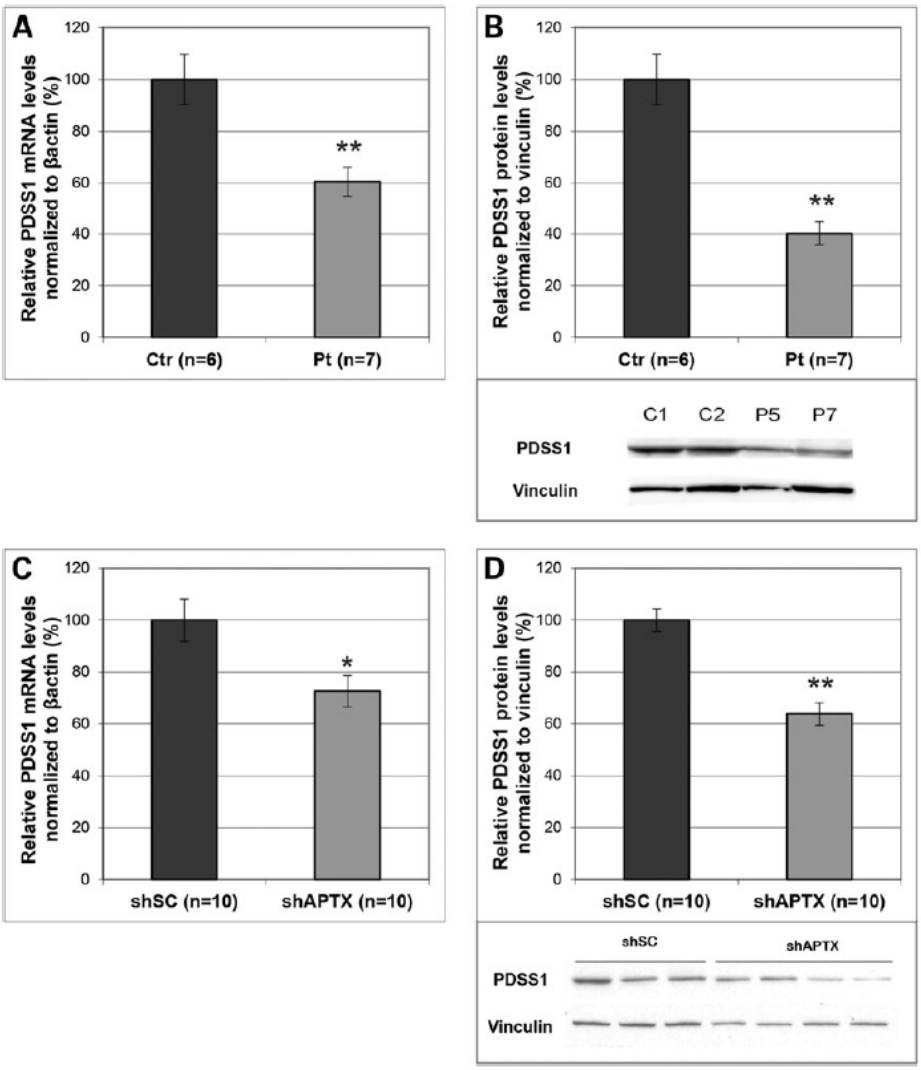


Figure 3. CoQ10 biosynthetic enzymes genes in APTX-mutant and APTX-depleted cells. mRNA expression level of CoQ10 biosynthetic enzymes genes in AOA1 fibroblasts with CoQ10 deficiency and APTX-depleted Hela cells. PDSS1 mRNA levels are decreased in AOA1 cells (A) and shAPTX (C), consistently with the reduction in PDSS1 protein levels (B and D). Representative PDSS1 western blot. Data are expressed as mean ± SEM in relative percentage of controls (*P < 0.05, **P < 0.01).

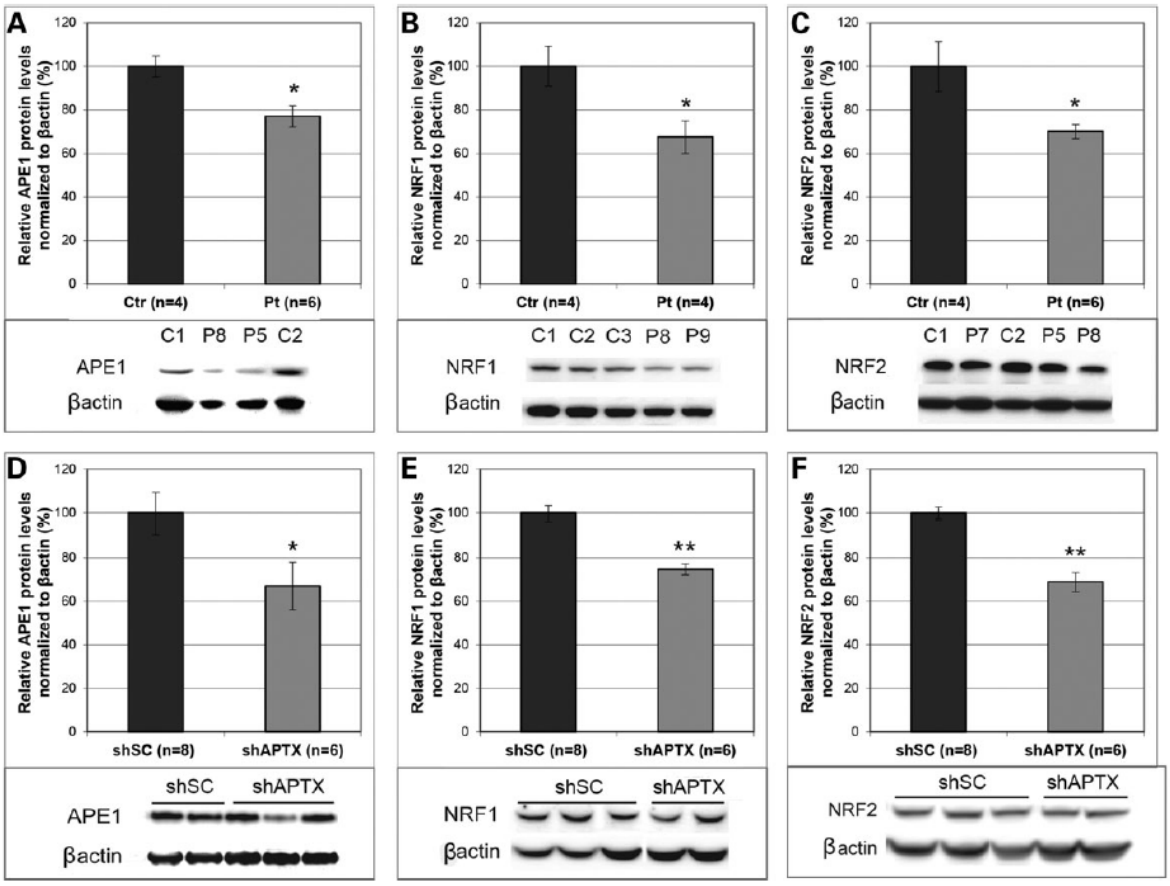


Figure 4. APE1, NRF1 and NRF2 in AOA1 fibroblasts and APTX-depleted Hela cells. APE1 (A and D), NRF1 (B and E) and NRF2 (C and F) protein levels are reduced in APTXmutant (A–C) and APTX-depleted cells (D–F). Representative western blot. Values are expressed as mean ± SEM in relative percentage of controls (*P < 0.05, **P < 0.01).

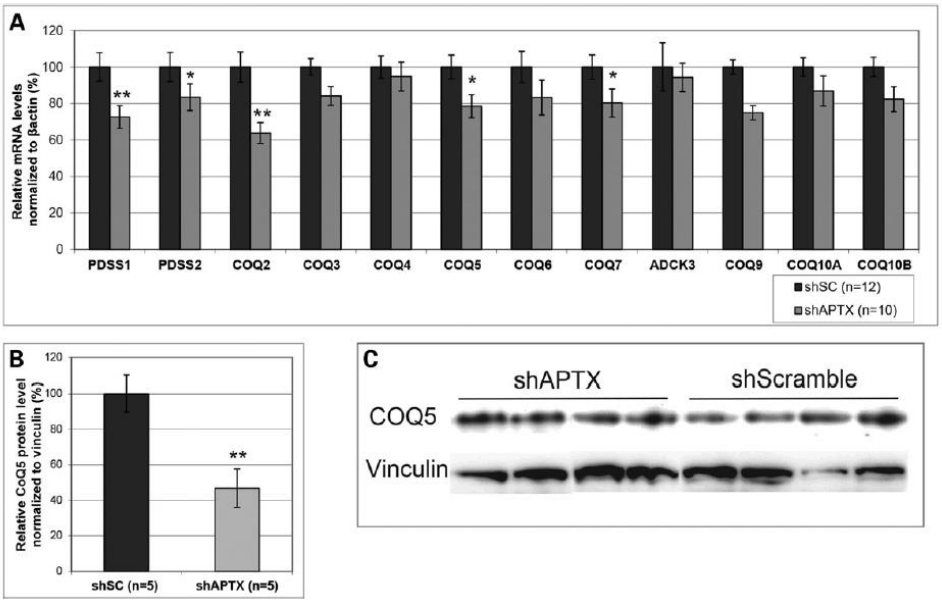


Figure 5. CoQ10 gene biosynthetic enzyme expression in APTX-depleted Hela cells. (A) PDSS1, PDSS2, COQ2, COQ5 and COQ9 are reduced in APTX-depleted cells. (B) COQ5 reduced expression was corroborated by decreased protein levels. (C) Representative western blot of COQ5. Values are expressed as mean ± SEM in relative percentage of control (*P < 0.05, **P < 0.01).

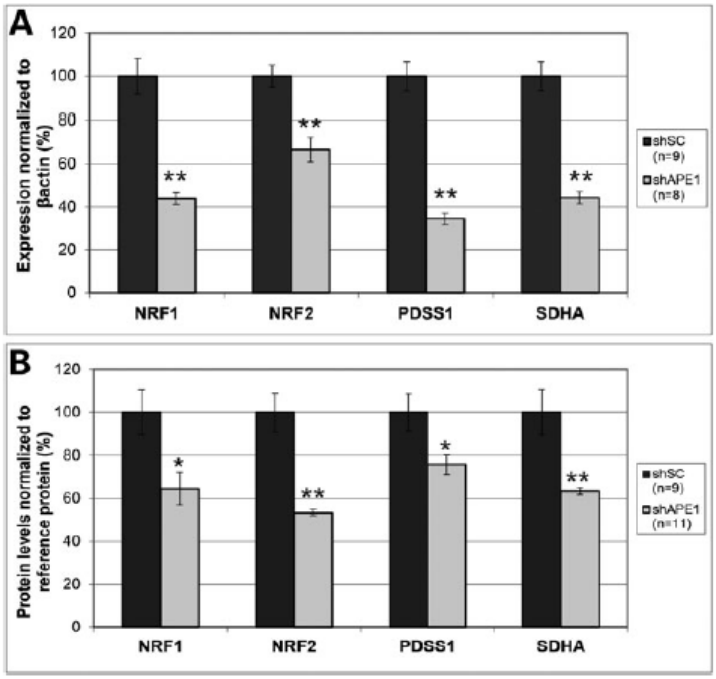


Figure 6. NRF1, NRF2, PDSS1 and SDHA levels in APE1-depleted cells. NRF1, NRF2, PDSS1 and SDHA mRNA (A) and protein levels (B) are decreased in APE1-interfered clones. Values are expressed as mean ± SEM in relative percentage of controls (*P < 0.05, **P < 0.01).

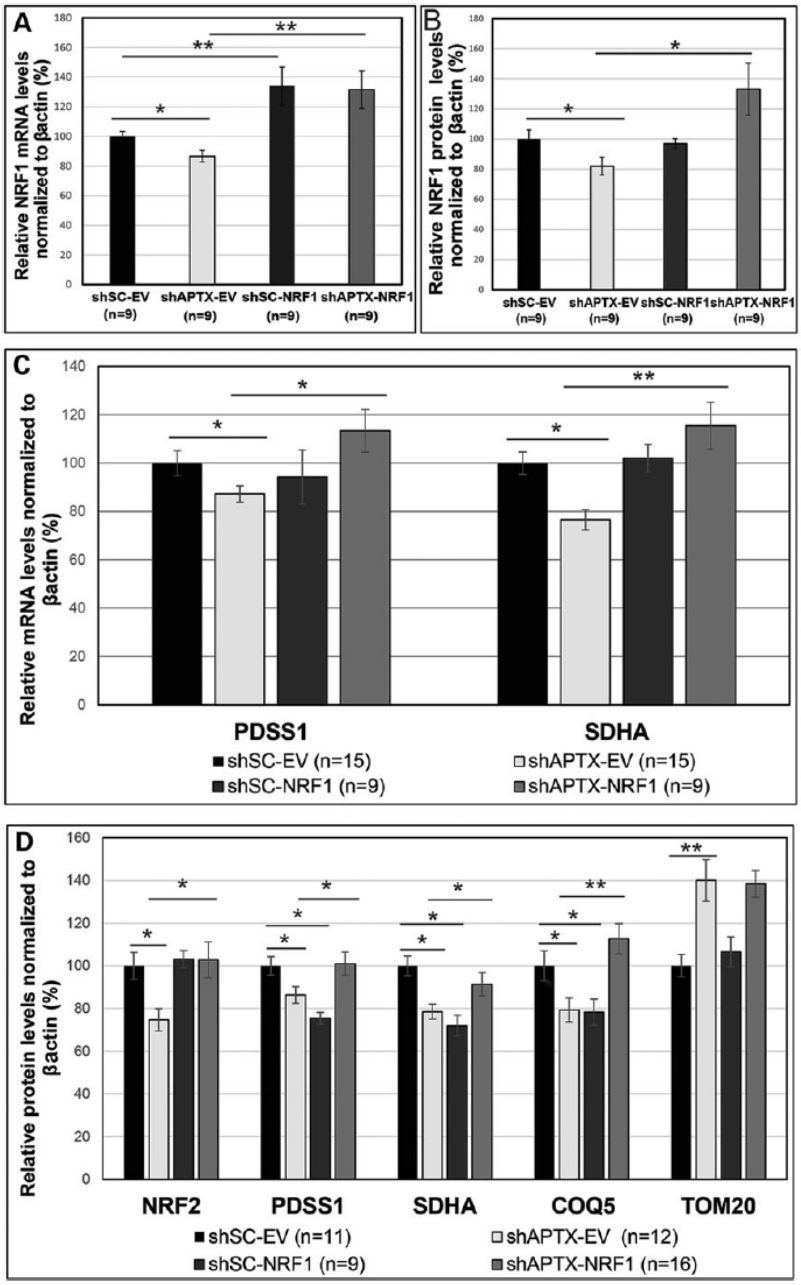


Figure 7. NRF1-expressing APTX-depleted Hela cells. Efficiency of NRF1 overexpression in APTX-depleted Hela cells assessed by the expression level of NRF1mRNA(A) and western blot to measure the level of NRF1 protein (B). Expression level of PDSS1 and SDHA mRNA (C), and protein level of NRF1, NRF2, PDSS1, SDHA, COQ5 and TOM20 (D). Values are expressed as mean ± SEM in relative percentage of controls (*P < 0.05, **P < 0.01).

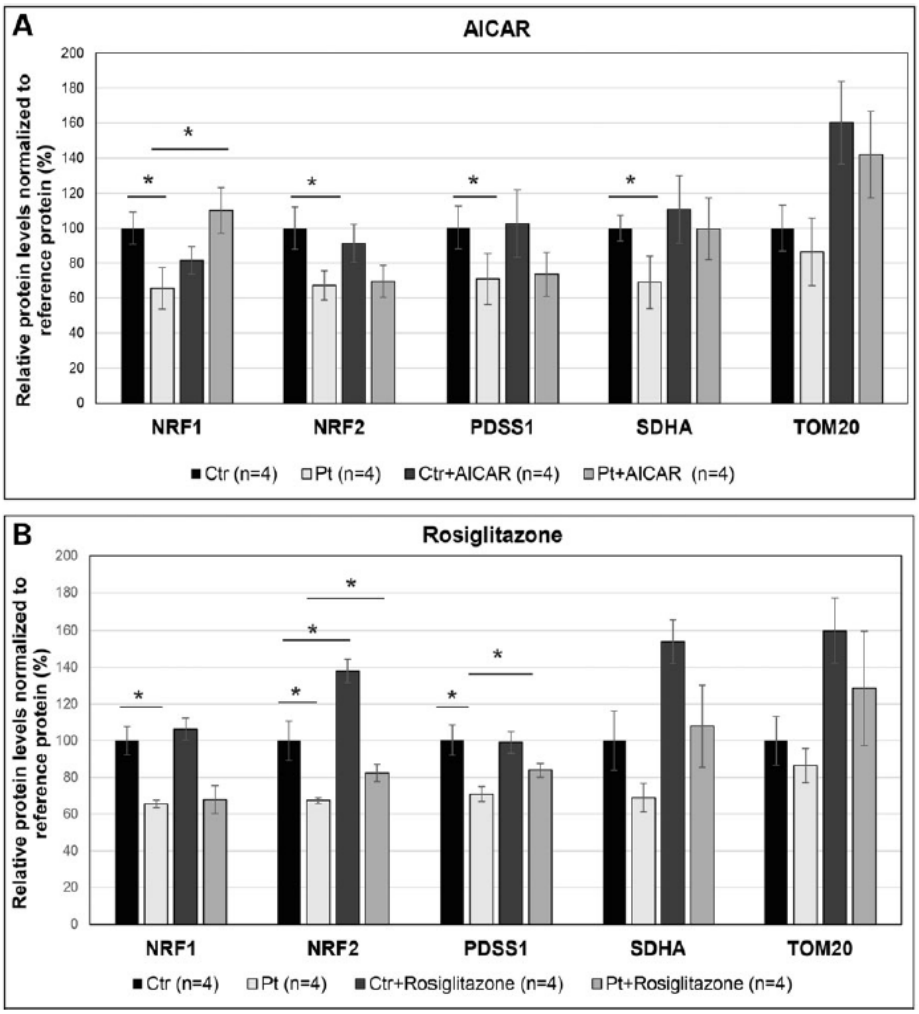


Figure 8. Effects of AICAR (A) and rosiglitazone (B) supplementation on NRF1, NRF2, PDSS1, SDHA and TOM20 levels (B), in AOA1 fibroblasts. Values are expressed as mean ± SEM in relative percentage of controls (*P < 0.05).